Journal of Power Sources 196 (2011) 7979–7984

Contents lists available at ScienceDirect

Journal of Power Sources

journal homepage: www.elsevier.com/locate/jpowsour

Macromolecular protic ionic liquid-based proton-conducting membranes for anhydrous proton exchange membrane application

Fuqiang Chu, Bencai Lin, Feng Yan*, Lihua Qiu, Jianmei Lu*

Jiangsu Key Laboratory of Advanced Functional Polymer Design and Application, Department of Polymer Science and Engineering, College of Chemistry, Chemical Engineering and Materials Science, Soochow University, Suzhou 215123, PR China

ARTICLE INFO

Article history:
Received 28 March 2011
Received in revised form 23 May 2011
Accepted 24 May 2011
Available online 31 May 2011

Keywords:
Ionic liquid
Polyamidoamine dendrimer
Polymer electrolyte membrane
Fuel cells

ABSTRACT

A type of anhydrous proton-conducting membranes are prepared via in situ cross-linking of polymerizable oils containing polyamidoamine (PAMAM) dendrimer-based macromolecular protic ionic liquids (PILs). The resultant composite membranes are transparent, flexible, and thermally stable up to 350 °C. Under anhydrous conditions, the macromolecular PIL-based membranes show proton conductivity of 1.2×10^{-2} S cm^{-1} at 160 °C, which is higher than that of the membranes containing small-molecule PILs. Furthermore, the macromolecular PIL-based composite membranes have much better PIL retention ability than which containing small-molecule PILs. These properties make this type of macromolecular PIL-based membranes suitable for high-temperature anhydrous polymer electrolyte membrane fuel cells.

© 2011 Elsevier B.V. All rights reserved.

1. Introduction

Polymer electrolyte membrane fuel cells (PEMFCs) are considered one of the promising power generation technologies that provide clean and efficient energy for vehicular transportation and portable devices applications [1,2]. PEMFCs have made great progress in recent decades, however, there are still some scientific and technological difficulties should be overcome before the widespread practical use. These issues mainly associated to the platinum catalysts and polymer electrolytes membrane used in the cells. PEM is one of the most important components in PEMFCs which acts not only as an electrolyte to transport protons, but also as a separator between the anode and cathode. The most commonly used PEMs, represented by humidified Nafion membranes, generally offer satisfactory fuel cell performance below 90 °C, however, cannot be used at higher temperatures because of the rapid evaporation of water, which results in a rapid loss of conductivity [3,4]. The operation of PEMFCs at elevated temperatures (>100 °C) could enhance the reaction kinetics at both electrodes, improve the carbon monoxide tolerance of the platinum catalyst at the anode, and simplify heat and water managements of cells [5]. Therefore, development of new types of PEMs with high conductivity at elevated temperatures is in great demand in the application of PEMFCs.

Several approaches have been pursued to obtain PEMs with high thermal stability and high conductivity at elevated temperatures under anhydrous conditions. These methods mainly include the synthesis of non-perfluorinated ionomer exchange membrane [6,7], incorporation of hydrophilic inorganic fillers into the PEMs for water retention enhancement [8,9], and the replacement of water with nonaqueous proton carriers, such as phosphoric acid [10] and protic ionic liquids (PILs) [11–15]. As one of the effective high-temperature proton carriers, PILs, have recently received much attention because of their negligible volatility, high proton conductivity, and excellent thermal stability [11–15]. Compared with Nafion membranes, PIL-based PEMs could be operated at temperatures above 100 °C under anhydrous conditions. However, long-term operation of PIL-based composite membranes generally suffered with a progressive release of the PIL components, and thus resulted in the decline of fuel cell performance [12,13]. To increase the performance and lifetime of PEMFCs, enhancing the PIL retention ability is in great demand. Our previous work already demonstrated that the addition of mesoporous silica nanospheres is an effective method in preventing the PIL release. However, excess addition of silica fillers declined the conductivity of membranes because silica nanoparticles themselves are much less conductive than PILs [13b].

Polyamidoamine (PAMAM) dendrimers are monodisperse, hyperbranched polymers with high concentration of primary and tertiary amine groups. This type of dendrimers can be readily protonated to form macromolecular cationic centers of PILs via neutralization with Brønsted acids. In addition, high surface charge density in higher generation PAMAM dendrimers leads to high proton conductivity [16]. The novel properties, including nonvolatile, good thermal stability, and high conductivity enable PAMAM-based

* Corresponding authors. Tel.: +86 512 65880973; fax: +86 512 65880089.
E-mail addresses: fyan@suda.edu.cn (F. Yan), lujm@suda.edu.cn (J. Lu).

0378-7753/$ – see front matter © 2011 Elsevier B.V. All rights reserved.
doi:10.1016/j.jpowsour.2011.05.064

macromolecular PILs as an effective proton carrier for anhydrous proton exchange membrane applications [16–18].

The objective of this study is to synthesize new PEMs based on macromolecular PILs with high proton conductivity at elevated temperatures. To achieve this aim, PEMs were synthesized via in situ cross-linking of polymerizable oils containing PAMAM-based macromolecular PILs. For comparison, PEMs containing small-molecule PIL were also synthesized and characterized under the same experimental conditions. The properties of the resultant composite membranes, such as proton conductivity, thermal stability, microstructure, and the PIL retention ability were investigated.

2. Experimental

2.1. Materials

The amine-terminated fourth-generation (G) PAMAM dendrimer (10 wt% in methanol) was purchased from Aldrich. Styrene, acrylonitrile, divinylbenzene (DVB), benzoin isobutyl ether, tetrahydrofuran, acetonitrile, diethyl ether, lithium bis(trifluoromethane sulfonyl)imide ($LiTf_2N$) and ethyl acetate were used as purchased. All the vinyl monomers were made inhibitor-free by passing the liquid through a column filled with base Al_2O_3. Distilled deionized water was used for all the experiments.

2.2. Synthesis

Protonated PAMAM G4.0-$NH_3^+HSO_4^-$ and PAMAM G4.0-$NH_3^+H_2PO_4^-$ were synthesized via neutralization with sulfuric and phosphoric acid, respectively. PAMAM G4.0-$NH_3^+Tf_2N^-$ was synthesized by the metathesis reaction of PAMAM G4.0-$NH_3^+HSO_4^-$ with $LiTf_2N$ in aqueous solution as documented in the literature [16,19]. PAMAM G4.0-$NH_3^+HSO_4^-$, ^{1}H NMR (500 MHz, D_2O), 3.62(t, $-CCH_2N-$), 3.51(br t, $-CONCH_2C-$), 3.32(br t, $-NCH_2C-$), 3.12(br t, $-CCH_2N-$), 2.82(br t, $-CCH_2CO-$). PAMAM G4.0-$NH_3^+H_2PO_4^-$, ^{1}H NMR (500 MHz, D_2O), 3.60(t, $-CCH_2N-$), 3.48(br t, $-CONCH_2C-$), 3.20(br t, $-NCH_2C-$), 3.09(br t, $-CCH_2N-$), 2.79(br t, $-CCH_2CO-$). PAMAM G4.0-$NH_3^+Tf_2N^-$, ^{1}H NMR (500 MHz, D_2O), 3.58(t, $-CCH_2N-$), 3.34(br t, $-CONCH_2C-$), 3.16(br t, $-NCH_2C-$), 2.97(br t, $-CCH_2N-$), 2.70(br t, $-CCH_2CO-$).

2.3. Preparation of PIL-based composite membranes

A mixture containing styrene/acrylonitrile (1:3 weight ratio, 60–95 wt%), PIL (5–40 wt%), DVB (2 wt% to the formulation based on the weight of monomer), and 1 wt% of benzoin isobutyl ether (photo initiator) was stirred and ultrasonicated to obtain a homogeneous solution, which was then cast into a glass mold and photo-crosslinked by irradiation with UV light of 250 nm wavelength for 30 min at room temperature.

2.4. Characterization

Thermal analysis was carried out on Universal Analysis 2000 thermogravimetric analyzer (TGA) with a temperature ramp of 10 °C min^{-1} under nitrogen flow. Phase-lag atomic force microscopy (AFM) images were measured using a NT-MDT Solver P47 AFM in a semicontact mode. The oscillation frequency was set to approximately 255 kHz with Si cantilever which had a spring constant of about 11.5 N m^{-1}. All AFM images were undertaken at room temperature.

The resistance of synthesized PIL-based polymer membranes was measured using the AC impedance method over the frequency range 1 Hz to 1 MHz on electrochemical workstations (Zahner IM6EX). A rectangular piece of membrane with the thickness of about 100 μm was sandwiched between two gold electrodes in a glass cell and placed in a programmable oven to measure the temperature dependence of the conductivity under anhydrous conditions. Composite membranes were dried at 100 °C for 8 h under a vacuum before the conductivity measurement in an effort to keep the samples dry. Before the measurements at each temperature set point, the samples were held at constant temperature for at least 10 min. The proton conductivity was obtained using the following equation:

$$\sigma = \frac{l}{RS}$$

where σ is the proton conductivity in S cm^{-1}, R is the ohmic resistance of the membrane, l is the distance between two electrodes, and S is the surface area of the membrane exposed to the electric field (cm^2).

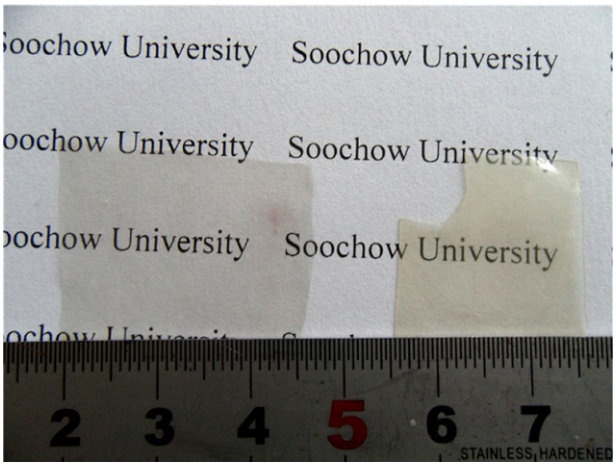

Fig. 1. Photograph of the polymer composite membranes containing 40 wt% PAMAM G4.0-$NH_3^+Tf_2N^-$ based.

3. Results and discussion

3.1. Structure characteristic of macromolecular PIL-based membranes

PAMAM dendrimer-based PILs were synthesized by neutralization of amine-terminated fourth-generation PAMAM dendrimers with corresponding Brønsted acids, as shown in Scheme 1A. Poly(styrene-co-acrylonitrile) has been recently used as the electrolytes for fuel cell because of its easy processing, excellent chemical, thermal stability and good mechanical properties [11–13,20]. Our previous work demonstrated that the chemical stability of cross-linked poly(styrene-co-acrylonitrile) is even comparative to that of Nafion-117 membranes if tested in Fenton's reagent [12]. Herein, poly(styrene-co-acrylonitrile) was again chosen as a polymer matrix for the preparation of macromolecular PIL-based PEMs. The PIL-based membranes were prepared via in situ photo-crosslinking of a mixture containing styrene, acrylonitrile, macromolecular PILs, and DVB in a glass mold (Scheme 1B). The resultant composite membranes containing 40 wt% macromolecular PILs are free-standing, transparent, and no apparent visible phase separation is observed during and after the polymerization process (Fig. 1). These membranes are flexible and can be cut into any desired sizes and shapes, whereas the pure form polymeric matrix (without PILs) is stiff and brittle.

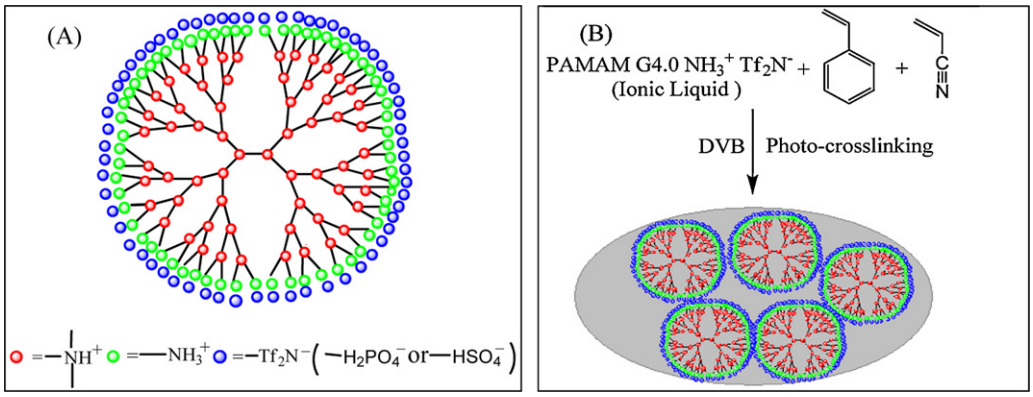

Scheme 1. (A) The schematic diagram of PAMAM G4.0-$NH_3^+Tf_2N^-$. (B) Reaction scheme for the preparation of PAMAM dendrimer-based PIL composite membranes.

3.2. Thermal stability

Fig. 2 shows the thermal stability of the synthesized macromolecular PILs and composite membranes containing macromolecular PILs examined with a thermogravimetric analyzer (TGA) at a temperature ramp of 10 °C min^{-1} under the nitrogen flow. It should be noted that pure PAMAM G4.0 dendrimer degraded at around 120 °C [21], while all the protonated PAMAM-based PILs lost less than 6% in weight up to 232 °C, about 110 °C higher than the PAMAM G4.0 dendrimer, indicating much better thermal stability of dendrimer-based PILs. The membranes containing 40 wt% macromolecular PILs lost less than 10% in weight up to 250 °C, confirming that this type of composite membranes indeed confer a high thermal stability, far beyond the range of interest for the application in PEMFCs.

3.3. Morphology

Fig. 3 shows the phase-lag atomic force microscopy (AFM) images of the fracture cross section of PIL-based composite membranes, revealing the morphology and distribution of macromolecular PILs in the composite membranes. Changes in the phase lag reflect changes in the mechanical properties of the sample surface such as composition, hardness, friction and viscoelasticity. Fig. 3A and C show the AFM phase images of the fracture cross-section of the composite membranes containing 5 wt% and 40 wt% of PAMAM G4.0-$NH_3^+Tf_2N^-$, respectively. In both two images, the brighter regions correspond to hard polymer domains, while the dark regions correspond to the soft PIL domains. Minimal correlation of AFM height images (Fig. 3B and D) indicates that phase-lag images (Fig. 3A and C) are unlikely to be an artifact of surface roughness. In the case of the membrane containing 5 wt% of macromolecular PILs, one can observe that the macromolecular PILs droplets with the diameter of ~30 nm (dark areas) are dispersed in a continuous polymeric matrix (bright areas), as shown in Fig. 3A. In Fig. 3C, 20–35 nm size of PIL with long and winding channels can be obtained. We believe that such a homogenously distribution and continuous PIL networks favor the formation of the proton transport channel, which therefore enhance the conductivity of the composite membranes.

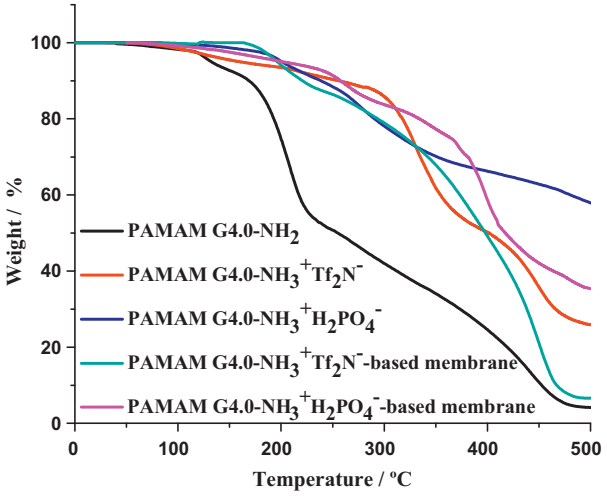

Fig. 2. TGA curves of PAMAM dendrimer-based PILs and polymeric membranes containing 40 wt% PILs. Heating rate: 10 °C min^{-1}.

3.4. Proton conductivity

Proton conductivity of PILs has recently been extensively studied and demonstrated by several research groups [5,11–15]. In the case of PAMAM G4.0-$NH_3^+H_2PO_4^-$-macromolecular PILs, $H_2PO_4^-$ forms hydrogen bonds with PAMAM G4.0-NH_3^+ and with $H_2PO_4^-$ themselves, as shown in Fig. 4. The proton conductivity probably originated from proton transfer along hydrogen-bond chains formed among $H_2PO_4^-$ themselves, which is in the same manner as other acid-polymer blends [5]. The proton conductivity of the composite membranes was measured with an alternating current impedance spectroscopy in a closed cell under anhydrous conditions. Fig. 5 shows the AC impedance spectra of different polymer membranes containing 40 wt% of PILs at 160 °C. For a membrane containing 5 wt% PAMAM G4.0-$NH_3^+HSO_4^-$, the conductivity is about 1.5×10^{-7} S cm^{-1} at room temperature under anhydrous conditions. Under the same experimental conditions, the membrane containing 40 wt% PAMAM G4.0-$NH_3^+HSO_4^-$ shows a conductivity of 1.5×10^{-4} S cm^{-1}. The conductivity of the composite membranes increases with an increase in the weight fraction of PILs (Fig. 6A). Furthermore, the membranes containing macromolecular PILs have higher proton conductivity values than the membranes containing small-molecule PIL, MIm[Tf_2N], probably because of the high surface charge density of the PAMAM dendrimer-based macromolecular PILs [16a]. Fig. 6B shows the temperature dependence of the proton conductivity of the composite membranes containing 40 wt% of macromolecular and small-molecule PILs, respectively. The conductivity of the resultant composite membranes increases with temperature increasing. The membrane containing 40 wt% PAMAM G4.0-$NH_3^+HSO_4^-$ shows the conductivity of 4.5×10^{-3} S cm^{-1} at 100 °C, and the value is increased to 1.2×10^{-2} S cm^{-1} at 160 °C.

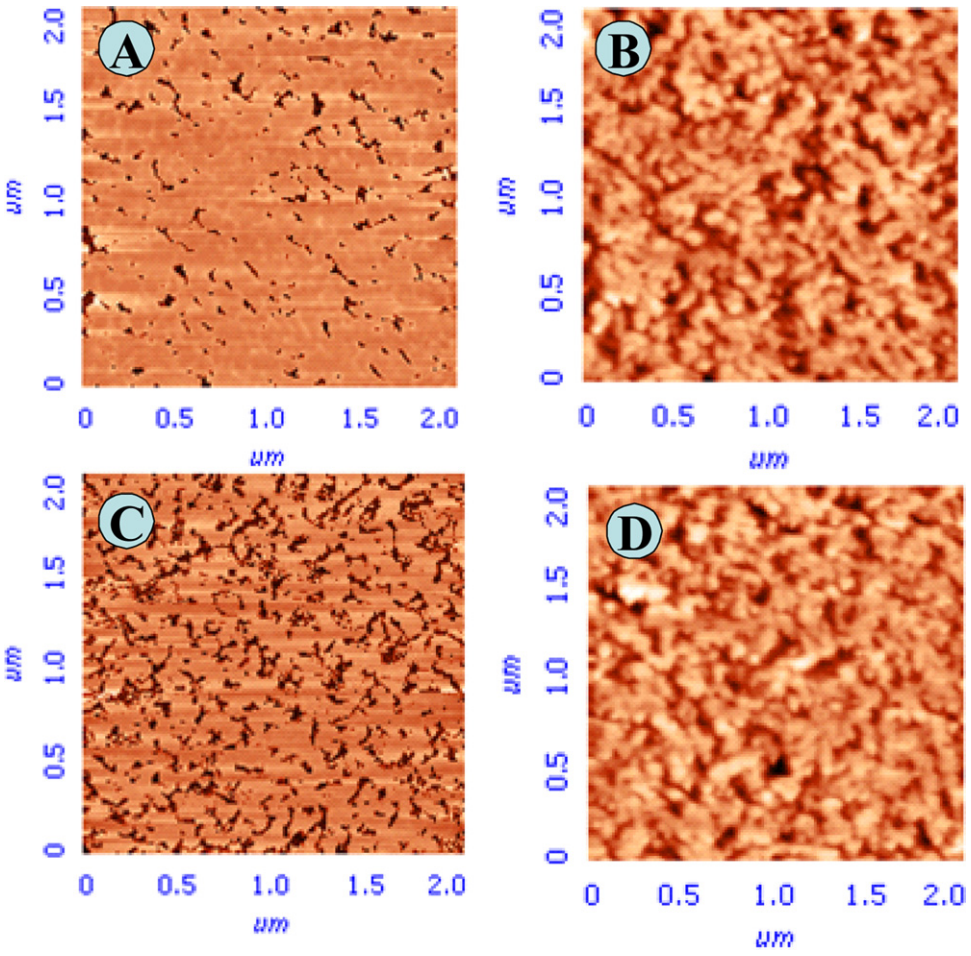

Fig. 3. AFM phase (A, C) and height (B, D) images of the fracture cross-section of PAMAM dendrimer-based polymer composite membranes containing 5 wt% PAMAM G4.0-$NH_3^+Tf_2N^-$ (A, B) and 40 wt% PAMAM G4.0-$NH_3^+Tf_2N^-$ (C, D). Each image frame is 2 μm × 2 μm.

The conductivity of this membrane is comparable to that of most reported small-molecule PIL-based polymer electrolytes at the same temperature region [12,13,22,23]. We believe that this relatively higher proton conductivity is mainly due to the high surface charge density of PAMAM-based macromolecular PILs, and the macromolecular PIL networks formed in the polymeric membranes. All the samples show no decay in conductivity at 160 °C.

3.5. Activation energy

The proton conductivity of PIL-based membranes obtained at elevated temperatures can be used for the estimation of activation energy (E_a) using the following equation [24]:

$$\ln \sigma = -\frac{E_a}{RT}$$

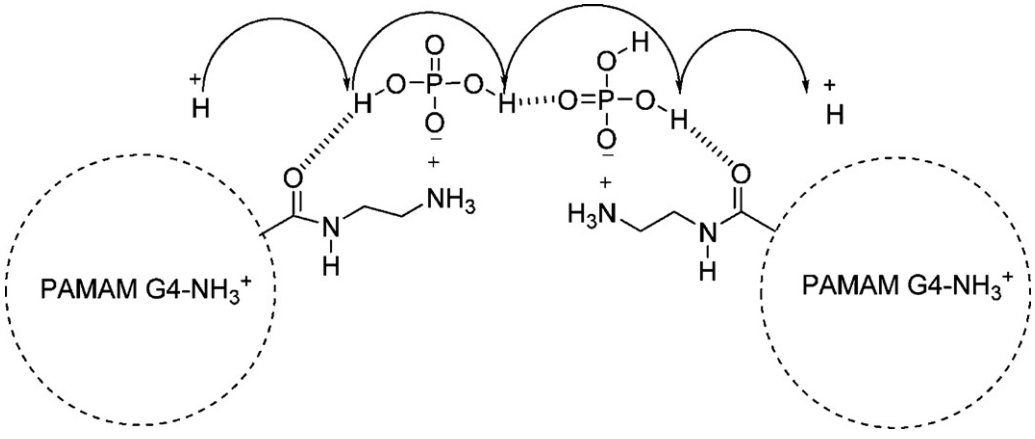

Fig. 4. The proton transport mechanism of PAMAM G4.0-$NH_3^+H_2PO_4^-$.

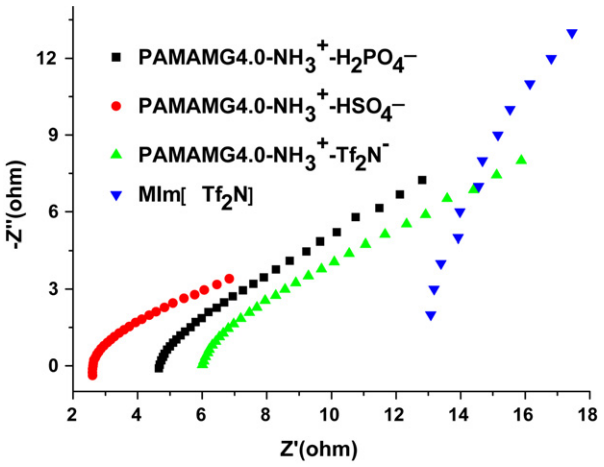

Fig. 5. AC impedance spectra of polymer membranes containing 40 wt% of PAMAM dendrimer-based PILs at 160 °C.

Table 1
Energy of activation (E_a) for PIL-based composite membranes.

Membrane	E_a (kJ mol^{-1})
40% PAMAM G4.0-$NH_3^+HSO_4^-$	16.0
40% PAMAM G4.0-$NH_3^+H_2PO_4^-$	18.7
40 wt% PAMAM G4.0-$NH_3^+Tf_2N^-$	19.9
40 wt% MIm[Tf_2N]	21.0
Nafion-117 [27,13a]	11.2–14.0

where σ is the proton conductivity in S cm^{-1}, E_a is the activation energy in kJ mol^{-1}, R is the universal gas constant (8.314 J (mol K)$^{-1}$) and T is the absolute temperature in K. The calculated E_a values are presented in Table 1. It can be seen that the changing trend of E_a values is related to the proton conductivity of membranes. The higher proton conductivity, the lower E_a values are. The membrane containing 40 wt% MIm[Tf_2N] has a higher E_a value compared with the membranes containing macromolecular PILs, indicating that proton transfer needs more energy in the membrane with small-molecule PILs. However, the E_a values of all the PIL-based membranes were higher than that of the Nafion-117 membrane saturated with water (11.2–14.0 kJ mol^{-1}) [25,26], showing that proton transfer needs more energy in the PIL-based composite membranes than Nafion-117. The proton conduction in PILs has been ascribed to a combination of proton hopping (Grotthuss) and vehicular mechanisms [27]. Based on the E_a values of the composite membranes, it can be concluded that proton transport of this type of macromolecular PIL-based membranes might have occurred by both mechanisms and predominantly by the hopping mechanism [12].

3.6. PIL retention ability of composite membranes

It is well to known that PILs are good replacements of water as proton carriers at elevated temperatures. However, the preventing progressive release of PIL component from the composite membranes during the fuel cell operation is still a great challenge [13a,b]. In this study, PIL retention ability of the composite membranes was confirmed by determining the weight loss of the samples after be immersed in the distilled water, as shown in Fig. 5A. In this work, composite membranes containing hydrophilic and water soluble PILs, MIm[BF_4] and PAMAM G4.0-$NH_3^+H_2PO_4^-$, and hydrophobic PILs, MIm[Tf_2N] and PAMAM G4.0-$NH_3^+Tf_2N^-$, were tested for comparison under the same experimental conditions, respectively. It is not surprise that the hydrophilic PIL-based composite membranes lost about 80 wt% of PILs in 40 min (Fig. 7A). However, it is worth noting the PIL retention ability of the macromolecular PIL-based membranes is much better than the membranes containing small-molecule PILs. For example, MIm[BF_4]-based composite membrane released about 90 wt% PILs within 30 min, while about 30 wt% PAMAM G4.0-$NH_3^+H_2PO_4^-$ was still kept in the composite membranes under the same experimental conditions. On the other hand, the PIL retention ability of the hydrophobic macromolecular PIL-based membranes is much better than that of hydrophilic PIL-based composite membranes. There is still 65 wt% of PAMAM G4.0-$NH_3^+Tf_2N^-$ be kept in the composite membrane even after be immersed in water for 2 h. These results indicate that the retention ability of macromolecular PIL-based composite membranes is much better than these containing small-molecule PILs. The factors that govern the PIL retention ability are not yet clearly understood. Our understanding is that it might be caused by the interactions (such as van der Waals interaction) between the polymeric matrix and macromolecular PILs. Compared with the small-molecule PILs, the bigger size of macromolecular PILs might also prevent the release from the composite membranes.

The PIL retention ability was further confirmed by the conductivity measurements of the water-extracted membranes. Fig. 7B shows that the conductivity of all the samples was dramatically decreased after the water-extraction treatment. The membranes containing PAMAM dendrimer-based macromolecular PILs show higher conductivity than these with small-molecule PILs. These results further confirm the better PIL retention ability of membranes containing macromolecular PILs than these with the small-molecule PILs.

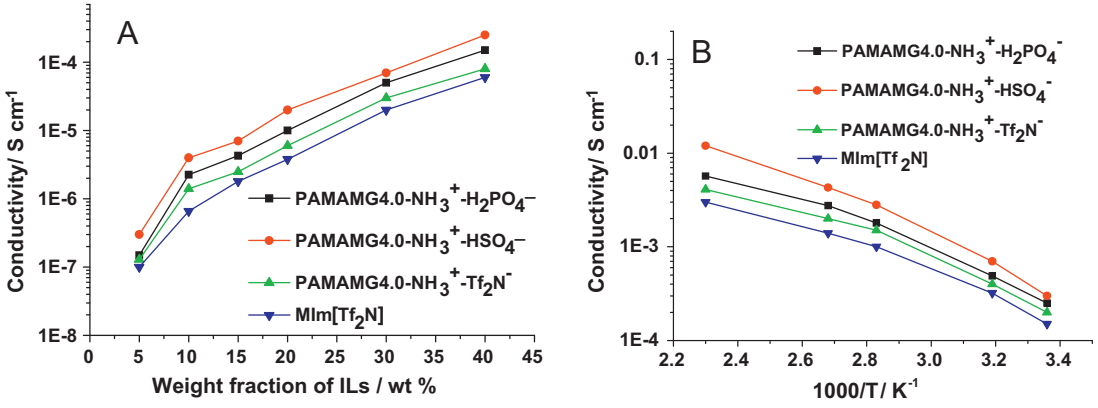

Fig. 6. Proton conductivity as a function of (A) weight fraction of PAMAM dendrimer-based PILs at 28 °C and (B) temperature for the polymer membranes containing 40 wt% PILs.

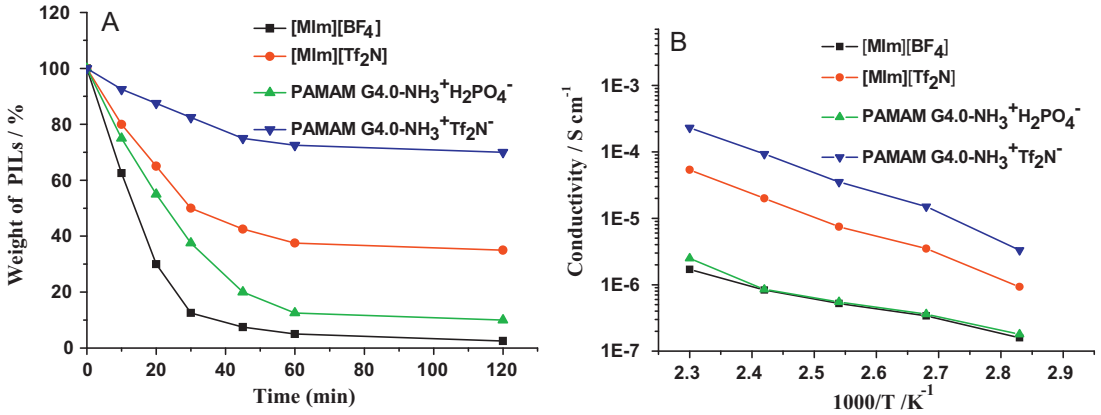

Fig. 7. (A) PIL retention ability test carried out in distilled water and (B) conductivity Arrhenius plots of various membranes after 50 min of water-extraction treatment. Each membrane containing 40 wt% PILs.

4. Conclusions

In summary, PAMAM dendrimer-based PIL/poly(styrene-co-acrylonitrile) composite membranes have been synthesized via in situ photo-crosslinking. The resultant macromolecular PIL-based composite membranes are free-standing, transparent, and show good thermal stability. Under anhydrous conditions, the produced composite membranes show the conductivity up to the order of 1×10^{-2} S cm^{-1} at 160 °C. The conductivity of the composite membranes increases with an increase in macromolecular PILs weight fraction. In addition, the membranes containing macromolecular PILs have much better PIL retention ability than that with small-molecule PILs. We believe this type of macromolecular PIL-based composite membranes should have an impact on further investigation in the field of anhydrous PEMs. However, further improvements to retain the PIL component upon fuel cell operation still need to be carefully considered. Design and synthesis of polymer matrices have strong interaction with PIL components might be one of the most effective ways to improve the PIL retention and will be further explored in our future work.

Acknowledgements

This work was supported by Natural Science Foundation of China (Nos. 20874071, 20974072), Research Fund for the Doctoral Program of Higher Education (20103201110003), The Program for New Century Excellent Talents in University (Grant NCET-07-0593), Fok Ying Tung Education Foundation (114022) and a Project Funded by the Priority Academic Program Development of Jiangsu Higher Education Institutions.

References

[1] M.Z. Jacobson, W.G. Colella, D.M. Golden, Science 308 (2005) 1901–1905.
[2] (a) B.C.H. Steele, A. Heinzel, Nature 414 (2001) 345–352;
(b) O. Diat, G. Gebel, Nat. Mater. 7 (2008) 13–14.
[3] H.F. Oetjen, V.M. Schmidt, U. Stimming, F. Trila, J. Electrochem. Soc. 143 (1996) 3838–3842.
[4] K.T. Adjemian, S.J. Lee, S. Srinivasan, J. Benziger, A.B. Bocarsly, J. Electrochem. Soc. A 149 (2002) 256–261.
[5] T. Tezuka, K. Tadanaga, A. Hayashi, M. Tatsumisago, J. Am. Chem. Soc. 128 (2006) 16470–16471.
[6] B. Bae, T. Yoda, K. Miyatake, H. Uchida, M. Watanabe, Angew. Chem. Int. Ed. 49 (2010) 317–320.
[7] M.L. Di Vona, E. Sgreccia, S. Licoccia, M. Khadhraoui, R. Denoyel, P. Knauth, Chem. Mater. 20 (2008) 4327–4334.
[8] Y. Jin, S. Qiao, L. Zhang, Z. Xu, S. Smart, J. Costa, G. Lu, J. Power Sources 185 (2008) 664–669.
[9] Y. Tominaga, I.C. Hong, S. Asai, M. Sumita, J. Power Sources 171 (2007) 530–534.
[10] (a) J. Weber, K. Kreuer, J. Maier, A. Thomas, Adv. Mater. 20 (2008) 2595–2598;
(b) Q. Li, J.O. Jensen, R.F. Savinell, N.J. Bjerrum, Prog. Polym. Sci. 34 (2009) 449–477.
[11] S. Subianto, M.K. Mistry, N.R. Choudhury, N.K. Dutta, R. Knott, Appl. Mater. Interfaces 1 (2009) 1173–1182.
[12] F. Yan, S. Yu, X. Zhang, L. Qiu, F. Chu, J. You, J. Lu, Chem. Mater. 21 (2009) 1480–1484.
[13] (a) A. Fernicola, S. Panero, B. Scrosati, J. Power Sources 178 (2008) 591–595;
(b) B. Lin, S. Cheng, L. Qiu, F. Yan, S. Shang, J. Lu, Chem. Mater. 22 (2010) 1807–1813;
(c) H. Diao, F. Yan, L. Qiu, J. Lu, X. Lu, B. Lin, Q. Li, S. Shang, W. Liu, J. Liu, Macromolecules 43 (2010) 6398–6405;
(d) J. Lu, F. Yan, J. Texter, Prog. Polym. Sci. 34 (2009) 431–448.
[14] N.J. Robertson, H.A. Kostalik, T.J. Clark, P.F. Mutolo, H.D. Abruna, G.W. Coates, J. Am. Chem. Soc. 132 (2010) 3400–3404.
[15] B. Lin, L. Qiu, J. Lu, F. Yan, Chem. Mater. 22 (2010) 6718–6725.
[16] (a) J. Huang, H. Luo, C. Liang, I. Sun, G.A. Baker, S. Dai, J. Am. Chem. Soc. 127 (2005) 12784–12785;
(b) T. Liu, C. Burger, B. Chu, Prog. Polym. Sci. 28 (2003) 5–26.
[17] Y.M. Chung, H.K. Rhee, Chem. Commun. (2002) 238–239.
[18] S. Antebi, P. Arya, L.E. Manzer, H. Alper, J. Org. Chem. 67 (2002) 6623–6631.
[19] D.A. Tomalia, H. Baker, J. Dewald, M. Hall, G. Kallos, S. Martin, J. Roec, J. Ryder, P. Smith, Macromolecules 19 (1986) 2466–2468.
[20] A. Silva, I. Takase, P.R. Pereira, A. Rocco, Eur. Polym. J. 44 (2008) 1462–1474.
[21] L. Balogh, A. deLeuze-Jallouli, P. Dvornic, Y. Kunugi, A. Blumstein, D.A. Tomalia, Macromolecules 32 (1999) 1036–1042.
[22] H. Nakajima, H. Ohno, Polymer 46 (2005) 11499–11504.
[23] A. Fernicola, S. Panero, B. Scrosati, M. Tamada, H. Ohno, ChemPhysChem 8 (2007) 1103–1107.
[24] X. Zhou, E. Weston, E. Chalkova, M.A. Hofmann, C.M. Ambler, H.R. Allcock, S.N. Lvov, Electrochim. Acta 48 (2003) 2173–2180.
[25] H. Pei, L. Hong, J.Y. Lee, J. Power Sources 160 (2006) 949–956.
[26] Y.S. Kim, M.A. Hickner, L. Dong, B.S. Pivovar, J.E. McGrath, J. Membr. Sci. 243 (2004) 317–326.
[27] A. Noda, M.A.B.H. Susan, K. Kudo, S. Mitsushima, K. Hayamizu, M. Watanabe, J. Phys. Chem. B 107 (2003) 4024–4033.